Nanotechnology **19** (2008) 195708 (6pp) doi:10.1088/0957-4484/19/19/195708

Side-by-side comparison of Raman spectra of anchored and suspended carbon nanomaterials

Anton N Sidorov[1], Santosh Pabba[1], Kapila P Hewaparakrama[2], Robert W Cohn[1] and G U Sumanasekera[1,2]

[1] ElectroOptics Research Institute and Nanotechnology Center, University of Louisville, Louisville, KY 40292, USA
[2] Department of Physics, University of Louisville, Louisville, KY 40292, USA

E-mail: gusuma01@louisville.edu

Received 29 January 2008, in final form 4 March 2008
Published 8 April 2008
Online at stacks.iop.org/Nano/19/195708

Abstract

Raman spectra of ordered carbon nanomaterials are quite sensitive to surface perturbations, including trace residues, structural defects and residual stress. This is demonstrated by a series of experiments with carbon nanotubes and graphene. Their spectra change due to subtle changes in preparation and attachment to the substrate and to each other. Differences are most clearly seen by forming a material into an air bridge and probing it in the air gap and at the anchor points. A monolayer graphene sheet, shows a larger disorder band at the anchor points than in the air gap. However, a bundle or rope of parallel-aligned single-wall nanotubes shows a larger disorder band in the gap than at the anchor points. For the graphene sheet the substrate surface deforms the graphene, leading to increases in the disorder band. For the rope, the close proximity of the nanotubes to each other appears to produce a larger stress than the rope resting on the substrate.

(Some figures in this article are in colour only in the electronic version)

1. Introduction

Ordered all-carbon nanomaterials such as carbon nanotubes (CNTs) and graphene monolayers have unique electrical, optical, thermal and mechanical properties [1, 2] that can be strongly affected by local environmental conditions. Interactions with the supporting substrate [3, 4] and surface adsorbates can obscure the intrinsic properties of these materials [4]. One way to eliminate substrate interactions is to suspend the material above the substrate, which also enables evaluation and application of their nanoelectromechanical properties [5, 6]. If the nanostructure is composed of multiple nanomaterials, van der Waals type interactions in some cases might be greater than substrate–nanomaterial interactions. In this report we use Raman spectroscopy to evaluate these type of interactions.

Raman spectroscopy is a sensitive probe of defects in carbon materials through defect-related changes in the D, D′ and G′ peaks. In a perfect sp^2 graphene network, the G band, which corresponds to the in-plane E_{2g} zone center phonon mode, is found at ∼1580 cm^{-1}. The disorder-induced D and D′ Raman features are generally related to defects such as curved graphite sheets, tube ends and finite-size crystalline domains and other carbonaceous (amorphous carbon) species. The G′ band (the overtone of the D band), which is always observed in defect-free graphene samples, arises due to the double-resonance (DR) Raman process, involving phonons within the interior of the first Brillouin zone of graphite. Here Raman spectroscopy is used to probe suspended monolayers of graphene and clusters of a few identical nanotubes (either single-or multi-wall) at their anchor points on the substrate and in the gaps.

Sample preparation may also introduce impurities and stresses which can influence the Raman spectra. In the method used to make nanotube air bridges, first a composite polymer–nanotube air bridge is formed, then the polymer is thermally decomposed [7]. We show there are significant differences in the Raman spectra of the nanotubes before and after decomposition, with stress and impurities contributing to

spectral features. Monolayer graphene is patterned between anchors without using any carrier material by an electrostatic deposition method [8].

Previously reported methods of suspending nanomaterials include (i) postgrowth assembly on pre-defined patterns [9], (ii) *in situ* CVD growth of SWNT networks over SiO_2 pillars, (iii) growth of CNTs on carbon nanofiber tip arrays [10] and synthesis of suspended SWNTs on Si inverse-opal templates by a chemical vapor deposition process [11]. These techniques have allowed systematic study of the effects of strain on the Raman properties of nanostructures, especially SWNTs, due to the interactions with the substrates. Previous studies of SWNTs by Raman spectroscopy show that the spectra change dramatically when they are (i) in bundles compared to isolated tubes [12], (ii) sitting on substrates compared to suspended between pillars as air bridges or in solutions [13] or (iii) contained in polymer composites [14–16]. None of these methods have addressed the situation where both nanotube–substrate and nanotube–nanotube interactions (in the absence of substrate) are simultaneously present, e.g. when a single rope of nanotubes is suspended. Also, recent Raman studies of graphene adsorbed on a substrate found that disorder bands become especially apparent for single monolayers, and that the strength of the disorder band is indicative of the thickness of graphene sheets up to several tens of monolayers thick [8, 17, 18]. Here we show that the magnitude of the disorder band in the suspended region is significantly reduced over the magnitude on the substrate, and the level is comparable to ∼7 layers of graphene [8] on a substrate.

2. Experimental details

Both SWNTs and MWNTs are non-covalently functionalized with an organic compound (trade name Kentera, Zyvex Corp., Richardson, TX) consisting of an alkane group connected to a phenyl end group that attaches to the nanotube and to an end group that enhances the solubility of the nanotubes in chlorobenzene. These functionalized nanotubes (which we refer to as f-nanotubes, or specifically f-SWNTs and f-MWNTs) are delivered dispersed in chlorobenzene, which is also a good solvent for poly(methyl methacrylate)—PMMA. Nanotube–PMMA solutions are made by adding PMMA (∼996 K) (15 wt%) to the nanotube solution (0.85 wt% in chlorobenzene) followed by sonication until a well-mixed suspension results. These nanotube and nanotube–PMMA solutions are used to make evaluation samples in the form of spun-on thin films on planar substrates and suspended fibers on a silicon micromachined array of pillars and air-dried. The composite solutions are hand brushed across the arrays of silicon pillars, following [7], which forms oriented, suspended nanofibers. Then, the polymer is thermally decomposed at 540 °C leaving air bridges of nanotubes. Suspended graphene bridges of from one to a few monolayers are fabricated by the method of electrostatic deposition from a freshly cleaved HOPG surface [8]. The Raman spectra are taken at room temperature with a Renishaw Invia Micro-Raman spectrometer in back-scattering geometry with laser excitation of wavelength 632.8 nm at a power level of 1.7 mW. The laser spot size at the sample is ∼1 μm^2. Raman spectra were obtained from 10 different locations for each material (SWNTs, MWNTs and graphene sheets) and each location was scanned five times to check for reproducibility.

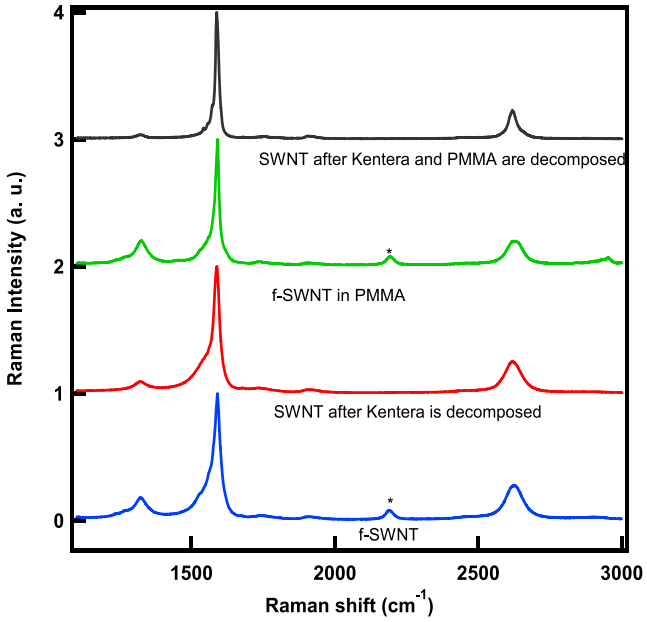

Figure 1. Raman spectra of SWNT thin films before and after thermal decomposition of the PMMA and functionalization. The peak corresponding to Kentera functionalization is identified by the symbol ∗.

3. Results and discussion

3.1. Raman spectra of the carbon materials

3.1.1. Raman study of nanotube thin films. Raman spectra are first collected of nanotube thin films on planar substrates. The purpose of this preliminary study is to demonstrate that the Kentera and PMMA are removed after heat treatment, leaving pure nanotubes, which are desired for the studies of the suspended nanotube air bridges. The f-nanotube and f-nanotube–PMMA suspensions are spun down onto substrates and the chlorobenzene evaporates to form thin films.

(i) SWNT–polymer composites. Figure 1 shows the Raman spectra of SWNT samples spun onto planar Si substrates before and after the removal of functionalization and PMMA. Each spectrum shows the D band at ∼1324 cm^{-1}, the G band at ∼1590 cm^{-1} and the G′ band at ∼2620 cm^{-1}, characteristic of SWNTs. The presence of a peak at ∼2190 cm^{-1} is associated with the Kentera since it disappears after thermal decomposition and the removal in thin films spun down with and without polymer. Lorentzian lineshape analysis [19] of the Raman spectra is used to calculate the ratio of areas of the D and G bands, D/G.

Table 1 shows that all the G and G′ modes upshift by ∼3 cm^{-1} when dispersed in Kentera and PMMA, presumably due to the compressive deformation inside the composite causing compression of the C–C bonds. Compression is also

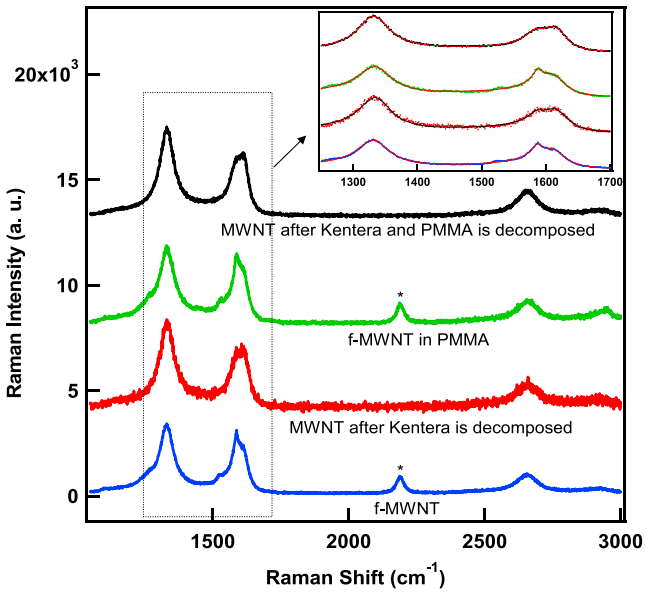

Figure 2. Raman spectra of functionalized MWNT and functionalized MWNT–PMMA before and after thermal decomposition. The peak corresponding to functionalization is identified by the symbol ∗. The inset shows an expanded view of the G, D and D′ bands with the best fits to multiple Lorentzians.

Table 1. Raman properties of SWNT thin films taken from the curves in figure 1.

Sample	D band (cm^{-1})	G band (cm^{-1})	G′ band (cm^{-1})	D/G ratio
f-SWNT	1324	1591	2626	0.07
SWNT after Kentera decomposes	1323	1588	2618	0.03
f-SWNT in PMMA	1324	1591	2628	0.05
SWNT after Kentera and PMMA decomposes	1323	1588	2619	0.01

consistent with the observed decrease in the D band to G band intensity ratio when Kentera and PMMA are removed by heat treatment. Interestingly, after heat treatment of the f-SWNT–PMMA, the intensity of the D band decreases even more than by heat treatment of the f-SWNT alone. This suggests that the defects in tube walls are mostly responsible for the D band compared to the amorphous carbon present in the sample. This is further supported by the presence of the narrower D′ band in the spectrum compared to all other spectra, presumably due to the changes in the resonance conditions for the double-resonance process. This phenomenon is not well understood at the moment and needs further investigation.

(ii) MWNT–polymer composites. Figure 2 shows the Raman spectra of MWNT samples spun onto planar Si substrates before and after the removal of functionalization and PMMA. Each spectrum shows the D band (∼1334 cm^{-1}), the G band (∼1588 cm^{-1}), the D′ band (∼1615 cm^{-1}) and the G′ (∼2656 cm^{-1}) band characteristic of MWNTs. We also observe the peak at ∼2190 cm^{-1} corresponding to functionalization for samples prior to thermal decomposition.

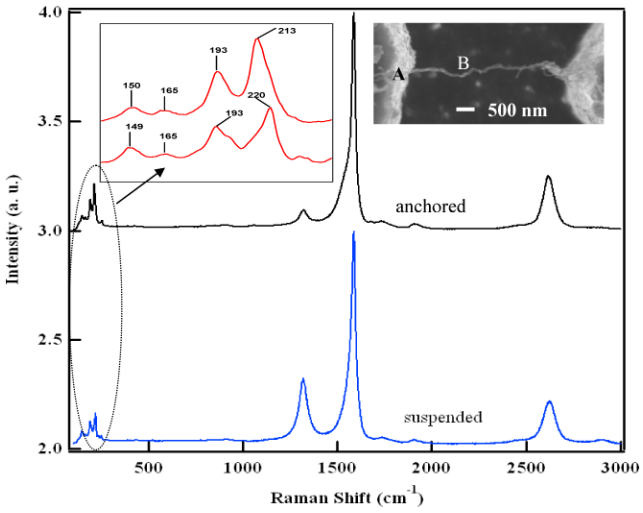

Figure 3. Raman spectra for suspended and anchored regions of the SWNT rope shown in the right inset. The left inset shows an expanded view of the RBM.

As shown in table 2, none of the peak positions show any appreciable systematic shifts due to the functionalization.

But the intensities of the G band, D band and D′ bands show systematic differences for the MWNT composites and polymer-free MWNTs. The MWNTs in both functionalization and PMMA show an intense G band compared to both D band and D′ band. After the removal of functionalization and PMMA, both the D band and D′ band become more intense than the G band. The formation of amorphous carbon residues during the thermal decomposition is believed to be responsible for the increased disorder band intensities.

3.1.2. Raman study of suspended nanotubes.

(i) SWNT air bridge. Raman signals from suspended individual SWNTs are shown to be easily measurable [20] since the signal intensities from nanotubes lying on the flat region of the Si pillar substrates are much weaker than those from the suspended SWNTs [13].

Figure 3 compares Raman spectra obtained from the regions of SWNTs on the top of the Si pillar (A) and in the gap (B) as shown in the inset. This structure is believed to be a single rope of SWNTs. The left inset to figure 3 shows the expanded view of the radial breathing mode (RBM) for the anchored and suspended SWNTs within the rope. The emergence of multiple RBM peaks in both spectra is indicative of the presence of several individual SWNTs in the rope as the RBM frequency (ω_r) is inversely proportional to the tube diameter (d). The tangential G band is observed at ∼1583 cm^{-1}. The disorder-induced D band, as well as the G′ band due to the double-resonance process, are seen at 1320 cm^{-1} and 2640 cm^{-1}, respectively. Figure 3 shows that the D/G ratio dramatically increases for the suspended portion of the rope compared to the SWNTs on the substrate. The D/G ratio for the suspended and non-suspended SWNTs are 0.18 and 0.01, respectively, presumably implying symmetry changes induced by the bending of the SWNTs. Other

Table 2. Raman properties of MWNT thin films taken from the curves in figure 2.

Sample	D band (cm^{-1})	G band (cm^{-1})	D′ band (cm^{-1})	G′ band (cm^{-1})	D/G ratio	D′/G ratio
f-MWNT	1333	1588	1613	2656	0.73	0.60
MWNT after Kentera decomposes	1334	1589	1617	2657	2.02	1.29
f-MWNT in PMMA	1334	1588	1615	2657	0.67	0.59
MWNT after Kentera and PMMA decompose	1333	1587	1617	2656	1.92	1.58

factors such as growth inhomogeneity of the SWNTs can also lead to similar results. Interestingly, the D/G ratio for the suspended region of the rope is higher than that of the thin films of f-nanotubes and f-nanotube–PMMA studied earlier. But the anchored part of the nanotube rope and the heat-treated thin films exhibit almost the same values of D/G. The Raman spectra indicate that the suspended SWNTs have higher D/G ratio than the SWNTs sitting on the flat substrate surface, consistent with the observations by Kobayashi *et al* [13]. This anomalous behavior is further accompanied by the upshifting of the most intense RBM in the suspended part of the SWNT rope (220 cm^{-1}) compared to that of the anchored part (213 cm^{-1}). It has been theoretically predicted that, in bundled SWNTs, van der Waals interaction between the SWNTs in the bundle causes ∼10% upshift of RBM frequencies compared to isolated ones [13]. This is consistent with the fact that the tube–tube interaction within the suspended part of the rope is stronger compared to that in the anchored part. The decomposition process used to remove polymer from the bridge may also tend to cause differences in the Raman spectra. The heating first melts the polymer, causing the nanotubes in the air gap to be drawn together by capillary thinning forces. However, the polymer wets the surface in the anchor regions, causing the nanotubes to be spread against the substrate surface, decreasing the nanotube–nanotube interactions. Some evidence of capillary thinning is also evident in the tapered waist of the MWNT bridge in figure 4. The effects of the SWNT–substrate interaction and the laser heating can also play a role in the anomalies of the Raman spectra.

(ii) MWNT air bridge. Figure 4 shows the Raman spectra from the regions of the MWNTs suspended across Si pillars (A) and sitting on the substrate (B) as represented in the inset. The Raman spectra exhibit typical structure of MWNTs containing the Raman line at ∼1580 cm^{-1} corresponding to E_{2g} modes (G line) and additional lines at ∼1325 and ∼1612 cm^{-1} corresponding to the D line and D' line. Interestingly, the G band and the D′ band are well resolved for the suspended MWNTs with comparable D′ and G band intensities, but enhanced D/G intensity ratio (∼20). It can be seen that both the D band and the G′ band are narrower for the suspended MWNTs compared to their anchored counterparts. We again interpret this larger D/G ratio in the suspended MWNT network as due to the bending of the MWNTs and the stress arising due to the enhanced van der Waals interactions among individual nanotubes within the network.

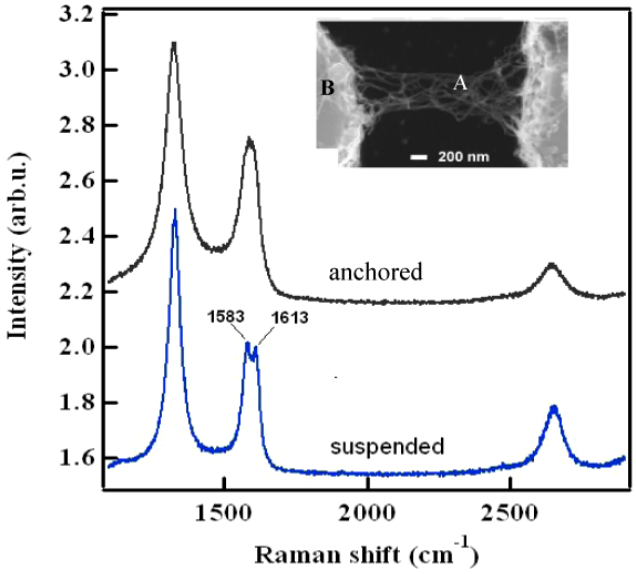

Figure 4. Raman spectra for suspended and anchored MWNTs across a Si pillar structure. The inset shows the MWNT network.

3.1.3. Raman study of suspended graphene. At first, suspended graphene bridges were fabricated by brushing graphene–PMMA solutions, followed by thermal decomposition of PMMA. Due to the limitations in the exfoliation process, this technique results in sheets that are several monolayers thick. However, for a sheet of n monolayers on a substrate, a single monolayer ($n = 1$) is known to have the largest D/G ratio [8]. Therefore the electrostatic deposition method, which can pattern a single monolayer, was used to produce a single monolayer that was probed by Raman spectroscopy.

The micro-Raman spectra of the graphene sheet are taken from three different locations as shown in the inset of figure 5. The presence of a single G′ band confirms that this is a monolayer of graphene [8]. It is interesting to observe that the D band intensity is minimum for the completely suspended graphene layer and maximum on the pillar. As expected, when the laser probe is centered on the edge of the pillar the D band is between the intensity of the suspended and anchored graphene. Further, the presence of a peak at ∼1620 cm^{-1} is observed for the graphene sheet lying on the pillar. This peak is seen to disappear for the suspended graphene. This band has been observed previously for monolayer graphene [8] and vapor grown carbon fibers [21] and has been attributed to the maximum in the phonon density of states associated with midzone phonons [22, 23]. The D/G ratio of the suspended monolayer is comparable to that of an $n = 7$ monolayer thick

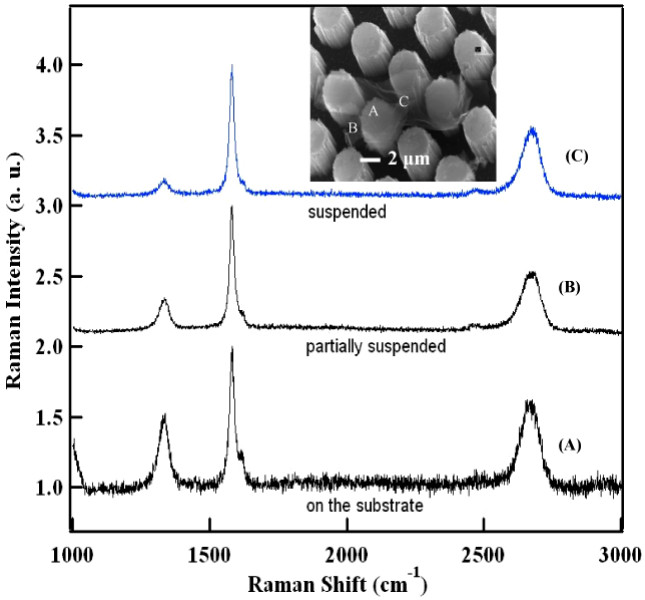

Figure 5. Raman spectra of suspended monolayer sheet of graphene. Spectra are shown for three different locations on the sheet indicated by (A), (B) and (C) in the inset. The D/G ratio of the suspended monolayer is comparable to that of an $n = 7$ monolayer thick sheet of graphene on a substrate in [8].

sheet of graphene on a substrate [8]. Note that in [8], with increasing numbers of monolayers, the D intensity became undetectable. The reason for the opposite trend of the D/G ratio for suspended and anchored parts for the nanotubes and the graphene sheets could relate to a different outcome of the surface interaction versus stress competition. A single-atom-thick sheet is thinner than a tube, and so much less stress across the structure is expected. It would also be interesting to see if the D band could be reduced further on the suspended graphene monolayer by further stressing or relieving stress, e.g. by bending or twisting the substrate.

4. Conclusions

The ability to make nanomaterial air bridges was used to enable side-by-side comparisons of the differences in Raman spectra due to whether the material is suspended or anchored. Compared to polymer-free SWNTs, the SWNTs dispersed in polymers show an upshift of the G and G′ bands and increased D/G ratio, which is consistent with compression of the C–C bonds of the SWNT by the polymer and increased disorder. The thermally decomposed MWNTs reflect increased disorder in the intensities of both D/G and D′/G ratios, implying the presence of amorphous carbon is responsible for the enhanced disorder. The suspended structures show intriguing Raman properties in relation to their structural variations. It is shown that both a suspended SWNT rope and an MWNT network show increased defect band intensities in the gap than on the anchor. This enhancement of the defect density in both suspended SWNTs and MWNTs is attributed to the stress arising due to the enhanced van der Waals interactions between suspended individual nanotubes In contrast, suspended graphene shows less disorder compared to the graphene adhered to a surface as the conformation of the monolayer graphene to the roughness of the surface produces structural defects.

Acknowledgments

This study was partially supported by the National Science Foundation grant ECS-0506941 and the National Aeronautics and Space Administration cooperative agreement NCC5-571.

References

[1] Geim A K and Novoselov K S 2007 The rise of graphene *Nat. Mater.* **6** 183–9
[2] Javey A, Shim M and Dai H 2002 Electrical properties and devices of large-diameter single walled carbon nanotubes *Appl. Phys. Lett.* **80** 1064–6
[3] Czerw R *et al* 2002 Substrate–interface interactions between carbon nanotubes and the supporting substrate *Phys. Rev.* B **66** 033408
[4] Cao J, Wang Q and Dai H 2005 Electron transport in very clean, as-grown suspended carbon nanotubes *Nat. Mater.* **4** 745–9
[5] Bunch J S, Van der Zande A M, Verbridge S S, Frank I W, Tanenbaum D M, Parpia J M, Craighead H G and McEuen P L 2007 Electromechanical resonators from graphene sheets *Science* **315** 490–3
[6] Franklin N R, Wang Q, Tombler T W, Javey A, Shim M and Dai H 2002 Integration of suspended carbon nanotube arrays into electronic devices and electromechanical systems *Appl. Phys. Lett.* **81** 913–15
[7] Pabba S, Sidorov A N, Berry S M, Yazdanpanah M M, Keynton R S, Sumanasekera G U and Cohn R W 2007 Oriented nanomaterial air bridges formed from suspended polymer-composite nanofibers *ACS Nano* **1** 57–62
[8] Sidorov A N, Yazdanpanah M M, Jalilian R, Ouseph P J, Cohn R W and Sumanasekera G U 2007 Electrostatic deposition of graphene *Nanotechnology* **18** 135301
[9] Takagi D, Homma Y and Kobayashi Y 2004 Selective growth of individual single-walled carbon nanotubes suspended between pillar structures *Physica* E **24** 1–5
[10] Hofmann S, Ducati C, Kleinsorge B and Robertson J 2003 Direct growth of aligned carbon nanotube field emitter arrays onto plastic substrates *Appl. Phys. Lett.* **83** 22
[11] Shi J, Lu Y F, Wang H, Yi K J, Lin Y S, Zhang R and Liou S H 2006 Synthesis of suspended carbon nanotubes on silicon inverse-opal structures by laser-assisted chemical vapour deposition *Nanotechnology* **17** 3822–6
[12] Dresselhaus M S, Dresselhaus G, Jorio A, Souza Filho A G and Saito R 2002 Raman spectroscopy on isolated single wall carbon nanotubes *Phys. Rev. Lett.* **40** 2043–61
[13] Kobayashi Y, Yamashita T, Ueno Y, Niwa O, Homma Y and Ogino T 2004 Extremely intense Raman signals from single-walled carbon nanotubes suspended between Si nanopillars *Chem. Phys. Lett.* **386** 153–7
[14] Kymakis E and Amaratunga A J 2006 Electrical properties of single-wall carbon nanotube–polymer composite films *J. Appl. Phys.* **99** 084302
[15] Bahun G J, Wang C and Adronov A 2006 Solubilizing single-walled carbon nanotubes with pyrene-functionalized block copolymers *Polym. Chem.* **44** 1941–51

[16] Wang W, Lin Y and Sun Y 2005 Poly(N-vinyl carbazole)-functionalized single-walled carbon nanotubes: synthesis, characterization, and nanocomposite thin films *Polymer* **46** 8634–40
[17] Ferrari A C *et al* 2006 Raman spectrum of graphene and graphene layers *Phys. Rev. Lett.* **97** 187401
[18] Gupta A, Chen G, Joshi P, Tadigadapa S and Eklund P C 2006 Raman scattering from high-frequency phonons in supported n-graphene layer films *Nano Lett.* **6** 2667–73
[19] Dresselhaus M S, Dresselhaus G, Saito R and Jorio A 2005 Raman spectroscopy of carbon nanotubes *Phys. Rep.* **409** 47–99
[20] Kobayashi Y, Takagi D, Ueno Y and Homma Y 2004 Characterization of carbon nanotubes suspended between nanostructures using micro-Raman spectroscopy *Physica* E **24** 26–31
[21] Zhang Y, Son H, Zhang J, Dresselhaus M S, Kong J and Liu Z 2007 Raman spectra variation of partially suspended individual single-walled carbon nanotubes *J. Phys. Chem.* C **111** 1983–7
[22] Chieu T C, Dresselhaus M S and Endo M 1982 Raman studies of benzene-desired graphite fibers *Phys. Rev.* B **26** 5867
[23] Saito R, Jorio A, Souza Filho A G, Dresselhaus G, Dresselhaus M S and Pimenta M A 2002 Probing phonon dispersion relations of graphite by double resonance Raman scattering *Phys. Rev. Lett.* **88** 027401